Small Angle X-ray Scattering by Simultaneous Interpenetrating Polymer Networks: Composition and Temperature Dependence

M. Junker and I. Alig*

Deutsches Kunststoff-Institut, Schlossgartenstrasse 6, D-64289 Darmstadt, Germany

H. L. Frisch

State University of New York at Albany, Department of Chemistry, Albany, New York 12222

G. Fleischer

Universität Leipzig, Fakultät für Physik und Geowissenschaften, Linnéstrasse 5, D-04103 Leipzig, Germany

M. Schulz

Universität Halle, Fachbereich Physik, D-06639 Halle, Germany

Received July 16, 1996; Revised Manuscript Received December 2, 1996[⊗]

ABSTRACT: The structure of simultaneously cross-linked interpenetrating polymer networks of poly(carbonate−urethane) (PCU) and poly(methyl methacrylate) (PMMA) has been studied by small-angle X-ray scattering (SAXS) with dependence on composition and temperature in a range from 298 to 373 K. At room temperature (298 K) the scattering intensity increases with decreasing scattering vector q and a q^{-4} dependence is found at large q values. The scattering profiles are compared with the Debye−Bueche theory for a statistical two-phase structure and a new recently developed hydrodynamic structure factor which describes the frustration of spinodal decomposition during the formation of simultaneous IPNs. Both approaches give the characteristic length of the frozen composition fluctuations between 2 and 35 nm for different compositions. With increasing temperature the scattering intensity of the sample with a characteristic length of 2 nm (60 wt % PCU) increases slightly at small q values. Above 353 K the scattering intensity increases tremendously and a maximum at q^* becomes evident. The corresponding length $l = 1/q^*$ increases by a factor of about 2 with increasing temperature. The maximum in scattering intensity cannot be described by the Debye−Bueche theory, whereas it is in agreement with the hydrodynamic structure factor. Several reasons for the irreversible changes above 353 K will be discussed and supported by field gradient NMR measurements on the same sample.

Introduction

Most of the polymers are known to be immiscible with one another, as a consequence of the small contribution from the mixing entropy of macromolecules to the free energy of mixing. One possibility to reduce the degree of phase separation and to combine the properties of different polymers is to form interpenetrating polymer networks (IPNs).[1,2] IPNs are composed of two (or more) chemically distinct networks held together predominantly by their trapped mutual entanglements rather than by covalent bond grafting. In the last decades a wide variety of IPNs have been synthesized (sequential, simultaneous, latex, gradient, thermoplastic, semi) and their physical properties and structures have been studied by different experimental methods including differential scanning calorimetry (DSC), mechanical measurements, electron microscopy, and scattering methods (SAXS, SANS).[3−7] From these investigations it is known that usually IPNs do not interpenetrate on a monomer scale but have a microheterogeneous morphology with regions enriched by segments of one of the components.

Recently, we published a combined theoretical and experimental investigation on a structure factor that was derived in the hydrodynamic limit which reflects the development of a microphase structure during the formation of a simultaneously cross-linked interpenetrating polymer network.[8] The structure formation was considered as a competitive process of spinodal decomposition and frustration of the fluctuations by topological restraints due to network growth. This structure factor shows a q^{-4} behavior at large scattering vectors q which is in agreement with the q^{-4} dependence of the Debye−Bueche theory[9,10] and Porod's law.[11] It is in contrast to the structure factor of fluctuations preceding phase separation in polymer blends[12] and microphase separation in homogeneous (ideal) IPNs[13] or block copolymers,[14] which shows a q^{-2} dependence at large scattering vectors q. Furthermore, for the IPNs considered a finite contribution to the structure factor is evident in the limit $q \rightarrow 0$ that is not expected for ideal IPNs and block copolymers. In the hydrodynamic theory this scattering contribution can be related to frustrated fluctuations.

Since the final structure of a simultaneous IPN can be considered as a frustrated highly nonequilibrium structure, originating from frozen spinodal fluctuations, it is expected that these structures can be equilibrated at higher temperatures and that changes of the interactions between the subnetworks with temperature can be detected. Therefore we performed temperature dependent X-ray scattering measurements and pulsed field gradient NMR on simultaneous IPNs of PCU and PMMA and have compared the results with the theory. The aim of this investigation is to get a deeper understanding of the nonequilibrium structure of real interpenetrating networks and to give further evidence for the agreement between the hydrodynamic theory and the experimental results.

* To whom the correspondence should be addressed.
[⊗] Abstract published in *Advance ACS Abstracts,* March 1, 1997.

S0024-9297(96)01046-7 CCC: $14.00

Experimental Section

Samples. The PCU/PMMA-IPN were synthesized under similar conditions as described in ref 15. The PCU network was prepared by cross-linking poly(1,6-hexanediol−carbonate) (PC) with biuret triisocyanate (BTI) derived from hexamethylene diisocyanate via an addition reaction. The PMMA network was synthesized simultaneously by a free radical reaction using ethylene glycol dimethacrylate (EGDMA) as a cross-linker and a mixture of benzoyl peroxide (BPO)/*N*,*N*-dimethylaniline (DMA) as an initiator redox system. From the molecular weight of the PC, $\bar{M}_w$ (PC) = 850, and the cross-linker used, $\bar{M}_w$ (BTI) = 500, the molecular weight between the cross-links $\bar{M}_c$ of the PCU network should be about 1180. The typical $\bar{M}_c$ of cross-linked PMMA is about 4000 as calculated from the employed stoichiometry and determined by swelling measurements. Samples with 30, 54, 60, 80 and 100 wt % PCU were investigated at room temperature (298 K). Temperature dependent measurements were performed on the sample with 60 wt % PCU.

SAXS Measurements. The SAXS measurements were performed with a Kratky Compact camera (A. Paar KG) equipped with a one-dimensional position-sensitive detector (M. Braun). Ni-filtered Cu Kα radiation (λ = 0.154 nm) was used. The samples were kept in the camera under vacuum to minimize air scattering. The data were corrected for absorption, background scattering, slit length smearing,[16] and thermal fluctuations.[17] Primary beam intensities were determined in absolute units (eu^2/nm^3) by using a moving slit method.

The relation between the absolute intensities $I(q)$ and the structure factor $S(q)$ is given by

$$I(q) = V_z \Delta\rho_e{}^2 S(q) \tag{1}$$

with the scattering vector q defined as

$$q = |\vec{q}| = \frac{4\pi}{\lambda}\sin(\theta) \tag{2}$$

λ is the wavelength of the X-rays ($\lambda_{\mathrm{Cu\ K\alpha}}$ = 0.154 nm) and 2θ is the scattering angle between the incident beam and the scattered radiation. V_z denotes the volume per monomer unit of PCU, which can be estimated from the molecular weight M and the density ρ of the pure PCU network (ρ(PCU) = 1.39 g/cm^3)

$$V_z = \frac{M}{\rho N_L} \tag{3}$$

to be V_z = 0.83 nm^3 (N_L = 6.02 × 10^{23} mol^{-1}). $\Delta\rho_e$ is the electron density difference between the IPN phases which is estimated from the experimental data by assuming a two-phase structure by numerical integration using[18]

$$\Delta\rho_e{}^2 = \frac{1}{2\pi^2 f(1-f)}\int_{q_{min}}^{q_{max}} I(q) q^2\, dq \tag{4}$$

(q_{min} = 0.12 nm^{-1}, q_{max} = 2.5 nm^{-1}, f is the composition ratio by weight). Values for $\Delta\rho_e{}^2$ are given in Table 1.

Field Gradient NMR Measurements. For the temperature dependent pulsed field gradient NMR measurements[19] a home-built spectrometer operating at a resonance frequency of 400 MHz has been used. The self-correlation function of the protons determined by this method is closely related to the incoherent scattering function in quasielastic neutron scattering experiments. For a two-component system the incoherent intermediate scattering function $S_{inc}(q',t)$ of the protons in the system is given in the diffusion limit for the stimulated echo experiment[19] by

$$S_{inc}(q',t) = A_1 \exp(-q'^2 D_1 t) + A_2 \exp(-q'^2 D_2 t) \tag{5}$$

with

$$A_i = \rho_i \exp(-2\tau/T_{2i}) \exp(-t/T_{1i}) \tag{6}$$

Table 1. Temperature Dependence of the Electron Density Difference $\Delta\rho_e{}^2$, Coefficients of $S(q)$ (Equation 18), and Characteristic Averaged Length l of IPNs

T (K)	$\Delta\rho_e{}^2$ (eu^2/nm^6)	$\bar{A}$	$10^{-2}\bar{m}$	$10^{-3}\bar{C}$	$10^5\gamma$	l (nm)
298	809	0.14	7.1	12.3	1.6	1.83
323	1261	0.25	3.7	13.3	3.8	2.09
333	1506	0.19	5.4	11.7	5.1	2.01
343	1502	0.19	5.8	10.9	7.4	2.03
353	1788	0.37	−0.6	9.8	10.2	2.48
363	1734	0.75	−1.0	2.5	80.8	4.17
373	3225	1.73	−10.1	3.0	27.2	4.92
298	1322	1.43	−7.0	2.7	14.8	4.79

Here the generalized scattering vector q' of NMR is given by $q' = \gamma\delta g$ with γ the gyromagnetic ratio of the proton, g the magnitude, and δ the width of the field gradient pulses. D_i are the self-diffusion coefficients (i = 1, 2) and T_{1i} and T_{2i} are the longitudinal and transverse relaxation times of the components supposed exponential relaxation, respectively. ρ_i is the spin density which is about the concentration of the component in the sample. The time τ is constant in one experiment, and q' is varied at a fixed diffusion time t, that is chosen according to the experimental conditions. The experimental results give an estimation about the mobilities of the different components and their fraction in the sample. In the case of IPNs nonreacted and other free small molecules can contribute to the signal with a finite self-diffusion coefficient D_1, whereas the fixed network chains and probably dangling ends contribute to the signal with D_2 close to 0. These chain segments are considered to diffuse less than several hundred nanometers for a given observation time $t \leq 50$ ms.

Structure of the Simultaneous IPN

Hydrodynamic Structure Factor. For the data analysis a recently developed structure factor for IPNs[8] was used, which reflects the frozen composition fluctuations due to spinodal decomposition during the formation of an IPN. This structure factor was derived in a hydrodynamic theory assuming that the simultaneous formation of two-component IPNs starts from the monomers, which form during the synthesis monotonously growing clusters with a given time dependent distribution. The evolution of the IPN is approximated on a (preaveraged) mean field level by effective hydrodynamic equations with time dependent coefficients. Since the experimental data are approximated by this theory, a short review of the basic assumptions and the meaning of the parameters has to be given. For each component the mass balance law holds in the hydrodynamic limit

$$\frac{\partial\rho_i}{\partial t} + \mathrm{div}\, j_i = 0 \tag{7}$$

(i = A, B). The current j_i can be described in a linear theory by $j_i = -\Lambda_{ik}\nabla\mu_k$ with the chemical potential μ_k and the generalized (nonlocal) Onsager coefficient Λ_{ik}. After introducing the order parameter $\psi(\vec{r}) = (1-f)\rho_A(\vec{r}) - f\rho_B(\vec{r})$ ($f = \langle\rho_A\rangle$, $1-f = \langle\rho_B\rangle$; f is the composition ratio), where $\rho_A(\vec{r})$ and $\rho_B(\vec{r})$ are the local concentrations of the two components at the point $\vec{r}$ and an effective current $j = (1-f)j_A - fj_B$ and $\mu = (1-f)\mu_A - f\mu_B$, respectively, Fourier transformation of eq (7) yields

$$\frac{\partial}{\partial t}\psi(q) = -q^2\Lambda(q)\mu(q) + \eta(q,t) \tag{8}$$

where η is added to the linear response term to represent thermodynamic noise corresponding to inner degrees of freedom. The free energy density F for a polymer mixture in terms of the order parameter ψ is

given by[12,20]

$$F = \frac{1}{N_A}\psi \ln \psi + \frac{1}{N_b}(1-\psi)\ln(1-\psi) - \chi\psi(1-\psi) + \frac{A}{2}|\nabla\psi|^2 \quad (9)$$

with the Flory−Huggins interaction parameter χ and $\sqrt{A}$ being the characteristic minimal length of the model (in the present case $\sqrt{A}$ is of the order of magnitude of the segment length). The effective chemical potential μ is the first derivative of F with respect to ψ. In linear approximation of the Fourier transform we get

$$\mu = \frac{\partial F}{\partial \psi(q)} \cong [Aq^2 + m]\psi(q) \quad (10)$$

where m is the inverse structure factor $\lim_{q\to 0} S^{-1}(q)$ which is proportional to $\chi_c - \chi$ and A is proportional to the gradient energy coefficient.

In the course of the chemical polymerization and cross-linking reactions during network formation, the mass and shape of the molecules and network fragments change. In the case of a distribution of molecules (cluster) A and m are effective values averaged over all molecules (we use the preaverage approximation). During chemical reaction mutual entanglements between the network clusters of the two components are expected to become evident. This suggests that an additional term C/q^2 has to be considered in eq 10 which describes the topological connections of the growing network.[21] Therefore in the simplest approximation A, m, and C become time dependent $A \rightarrow A(t)$, $m \rightarrow m(t)$, $C \rightarrow C(t)$ and describe the chemical evolution of the system. For IPNs the free energy is given by[12,22,23]

$$F = \int\left[Aq^2 + m + \frac{C}{q^2}\right]\psi(q)^2 \, \mathrm{d}^3q \quad (11)$$

$$\mu(q) = \left[A(t)q^2 + m(t) + \frac{C(t)}{q^2}\right]\psi(t) = L(q,t)\,\psi(t) \quad (12)$$

where $C(t)$ represents the local attractive interaction that becomes effective when the first closed network loops are formed and elastic forces start to counteract the repulsion of the two network components. The chemical potential μ from eq (12) and a simplified Onsager coefficient,[8] $\Lambda = D_0 f(1-f)$, assuming Rouse dynamics,[24] where D_0 is the segmental diffusion coefficient, can now be substituted into eq (8). The solution of the differential eq is then given by

$$\psi(t) = \int_0^t\{-q^2 D_0 f(1-f)\int_\tau^t L(q,t')\,\mathrm{d}t'\}\eta(q,\tau)\,\mathrm{d}\tau \quad (13)$$

For the kinetics of the chemical reactions taking place during the IPN formation a finite time $t = t_c$ can be defined above which the separation kinetics of the IPN is suppressed, which is assumed to be close to the gel time t_{gel}. Above this time the evolution of the separation kinetics is frozen and $\psi(t)$ becomes a static value $\psi_s = \psi(t)$:$t > t_c$. From this solution the structure factor $S(q)$ of the irreversible frozen fluctuations can be calculated as

$$S(q) = \langle\psi(q,t)^2\rangle = \int_0^{t_c}\int_0^{t_c}\exp\{-q^2 D_0 f(1-f)\int_\tau^{t_c} L(q,t')\,\mathrm{d}t' - q^2 D_0 f(1-f)\int_{\tau'}^{t_c} L(q,t')\,\mathrm{d}t'\}\langle\eta(q,\tau)\,\eta(q,\tau')\rangle\,\mathrm{d}\tau\,\mathrm{d}\tau' \quad (14)$$

By Employing the equipartition theorem for the thermodynamic noise and by use of the mean value law for the integration, the structure factor $S(q)$ of the irreversibly frozen fluctuations is given by[8]

$$S(q) = \frac{1-\exp(-\gamma L(q)q^2)}{q^2 L(q)} = \left[1 - \exp\left(-\gamma\frac{q^2}{S_0}\right)\right]\frac{S_0}{q^2} \quad (15)$$

with

$$S_0 = \frac{1}{\bar{A}q^2 + \bar{m} + \frac{\bar{C}}{q^2}} \quad (16)$$

in which $\bar{A}$, $\bar{m}$, and $\bar{C}$ are time-averaged effective values. γ is an effective coefficient which depends on the diffusion coefficient of the monomers, the composition ratio, and the kinetics of the IPN formation determined by t_c.

It should be noted that, as a result of using the mean value law for integration in the derivation of the structure factor $S(q)$, the values of the coefficients $\bar{A}$, $\bar{m}$, and $\bar{C}$, and γ differ from their actual values at time $t = t_c$, when the composition fluctuations are frozen. They represent effective mean values which depend on the thermodynamic history of the sample. Thus a simple physical interpretation of the coefficients is rather difficult. However, in contrast to the MST theories for homogeneous (ideal) IPNs the time dependent structural evolution during network formation is taken into account, which seems to be necessary for real IPNs.[25]

The coefficients of S_0 determine an averaged characteristic length

$$l = \frac{1}{q^*} = \left(\frac{\bar{A}}{\bar{C}}\right)^{1/4} \quad (17)$$

that represents the structural evolution during network formation. The structure factor $S(q)$ given in eq 15 reveals a q^{-4} dependence at large q values in contrast to the structure factor for a phase separation in ideal IPN which shows a q^{-2} dependence.[13]

Although the theory is originally developed for isothermal formation of a simultaneous IPN, the parameters can also be interpreted for different temperatures. Since the chemical reaction can be performed at different temperatures, the kinetics of the structural evolution can be described by time and temperature dependence of the coefficients $\bar{A}$, $\bar{m}$, and $\bar{C}$, and γ. The time t_c when the structure is frozen is also temperature dependent. For isothermal network formation $S(q)$ characterizes the frozen structure at a certain temperature T_1. If the temperature after the reaction ($t > t_c$) is changed to T_2, a further development of the nonequilibrated structure can occur, which may be represented by additional changes in the structure factor in terms of the integration of additional composition fluctuations between the limits $t_c(T_1)$ and $t_c'(T_2)$. The changing structure is then frozen at time $t_c'(T_2)$, and the values of the coefficients $\bar{A}'$, $\bar{m}'$, and $\bar{C}'$, and γ' determined from the fit of the scattering data are new effective mean values, which include the whole ther-

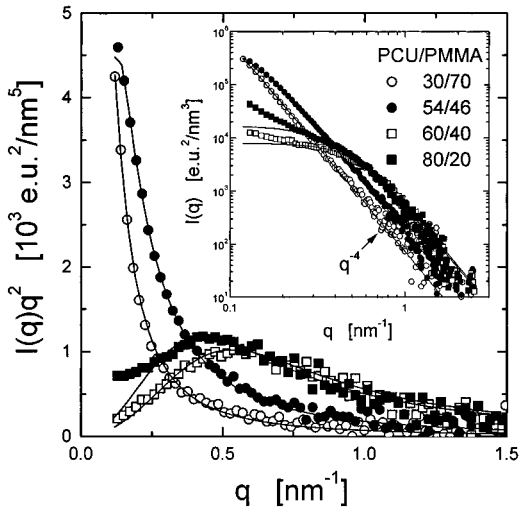

Figure 1. Scattering intensity $I(q)q^2$ versus scattering vector q of PCU/PMMA-IPNs at $T = 298$ K. The lines are fits with the hydrodynamic theory. The inset shows a log−log plot of the scattering intensity $I(q)$ versus q and the fits using the Debye−Bueche theory. The fit functions are explained in the text.

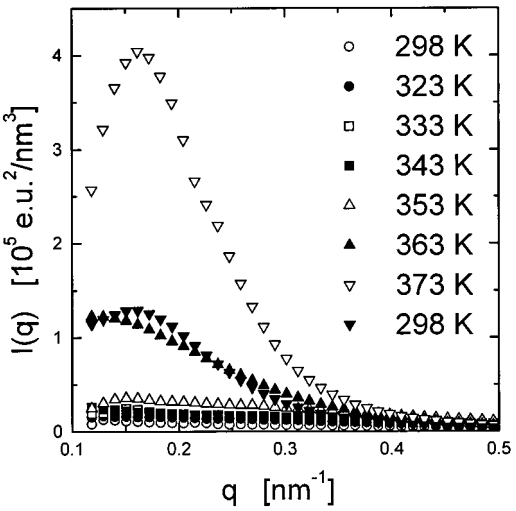

Figure 2. Temperature dependence of the scattering intensity $I(q)$ versus scattering vector q of PCU/PMMA-IPN with 60 wt % PCU.

modynamic history of the sample. It should be noted that the time $t_c'(T_2)$ is not identical to the characteristic time t_c for isothermal reaction at temperature T_2, since the reaction kinetics is of course different for both cases.

Debye−Bueche Theory. In previous scattering experiments on IPNs[26] the scattering data were analyzed by a statistical approach using the structure factor of Debye−Bueche[9,10]

$$S_{DB}(q) = \frac{S(0)}{(1 + \xi^2 q^2)^2} \tag{18}$$

which assumes a random distribution of phases with different sizes and shapes. A correlation function $\gamma(r)$ is used to describe structural features. For a multiphase system it gives the probability that two points separated by a distance r will still be in the same phase. In the Debye−Bueche approach an exponential correlation function is used

$$\gamma(r) = \gamma(0) \exp(-\xi/r) \tag{19}$$

with the correlation length ξ. The structure factor $S_{DB}(q)$ shows a q^{-4} dependence at large q values in accordance with Porod's law for a two-phase system with sharp phase boundaries.[11]

Results and Discussion

Figure 1 shows the composition dependence of the scattering intensity $I(q)q^2$ versus scattering vector q which has been discussed more in detail before together with the development of the hydrodynamic structure factor $S(q)$.[8] The $I(q)q^2$ versus q representation is suggested by eq 15 from the hydrodynamic theory. The experimental data are in good agreement with the theory, and the averaged characteristic length l can be determined according to eq 17. The inset shows a log−log plot of the scattering intensities $I(q)$ versus scattering vector q and the fits using the structure factor by Debye−Bueche $S_{DB}(q)$ which are also in good agreement with the data. The averaged characteristic length of the frozen fluctuations at room temperature was found to be about 2 nm for samples having one thermodynamic glass transition (60 and 80 wt % PCU) and between 15 and 35 nm for samples having two glass transitions (30 and 54 wt % PCU). The scattering profiles show a q^{-4} behavior at large q values in accordance with both theories. A clear distinction between the two theories was not possible from this result. However, the hydrodynamic theory of course considers structural evolution of the microphases during IPN formation, whereas the Debye−Bueche theory gives a very general description of the final structure.

The influence of temperature on the scattering intensity $I(q)$ has been investigated for the sample with 60 wt % PCU which has a small characteristic length of about 2 nm at 298 K. The scattering profiles are shown in Figure 2 for different temperatures between 298 and 373 K. The samples are heated by starting at room temperature and holding the temperature constant for 3 days at each temperature before measuring the q dependence of the scattering intensity. After heating to 373 K, the sample was cooled to room temperature and a second measurement was performed at 298 K after 3 days. Up to a temperature of 353 K the scattering intensity $I(q)$ only changes slightly with temperature, whereas $I(q)$ increases tremendously between 353 and 373 K and a well-resolved maximum becomes evident. After the sample is cooled to 298 K, these changes in $I(q)$ are not fully reversed. The remaining scattering intensity is similar to that at 363 K with a well-resolved maximum.

The log−log plots of intensity $I(q)$ versus q are shown in Figure 3. The scattering profiles of all temperatures show a q^{-4} dependence at large q values with a slight deviation at very high q values. The latter may be due to difficulties of background subtraction. This behavior at high or intermediate q values corresponds to the well-known Porod law.[11] For all temperatures a finite contribution to the scattering intensity for $q \rightarrow 0$ is evident. A reasonable fit of the Debye−Bueche law[9] to the data as suggested before[26] was only possible for the data below 353 K and cannot explain the maximum in $I(q)$ versus q at higher temperatures.

Figure 4 shows the scattering data as $I(q)q^2$ versus q. In this plot a maximum at q^* is expected from the hydrodynamic theory (see eqs 16 and 17). The scattering profiles show the expected maximum in the scattering intensity for all temperatures, where a strong increase with temperature is evident above 353 K. As discussed before, a higher scattering intensity remains

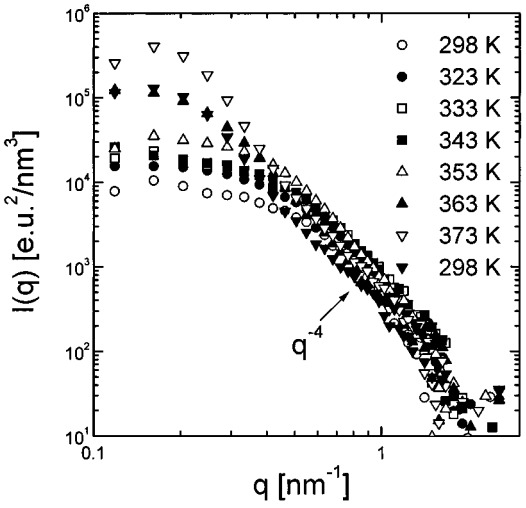

Figure 3. log−log plots of scattering intensity $I(q)$ versus scattering vector q of PCU/PMMA-IPN with 60 wt % PCU.

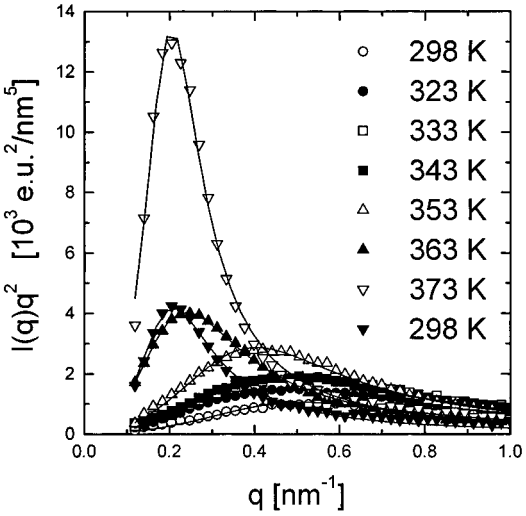

Figure 4. Temperature dependence of scattering intensity $I(q)q^2$ versus scattering vector q of PCU/PMMA-IPN with 60 wt % PCU. The lines are fits by the hydrodynamic structure factor $S(q)$ (eq (15)).

after cooling the sample to 293 K. The position of the maximum in $I(q)q^2$ is almost constant for $T \leq 253$ K and shifts drastically at 263 K and 273 K to smaller values of q^*. The fits of the data by the hydrodynamic structure factor $S(q)$ (eq (15)) are also given in Figure 4. The coefficients $\bar{A}$, $\bar{m}$, $\bar{C}$, and γ of the best fits and the characteristic length l (see eq (17)) are listed in Table 1.

The averaged characteristic lengths are plotted versus temperature in Figure 5. The length is only slightly increasing up to 353 K and becomes a factor of about 2 larger for temperatures above 353 K. We speculate that this large change above 353 K is related to the glass transition temperature measured for a pure PMMA network. Although the PCU/PMMA-IPN with 60 wt % PCU shows a fine microphase structure having a characteristic length of about 2 nm, only one glass transition was found by DSC at $T_g = 276$ K. One can thus expect unfreezing of the PMMA segments on a scale that is smaller than the correlation length of the calorimetric glass transition for a pure PMMA network. This small scale glass transition can deviate from that of the bulk material, as suggested before by two of us.[27] It was pointed out that a frustration of the glass transition can lead to a decrease in T_g. Another reason-

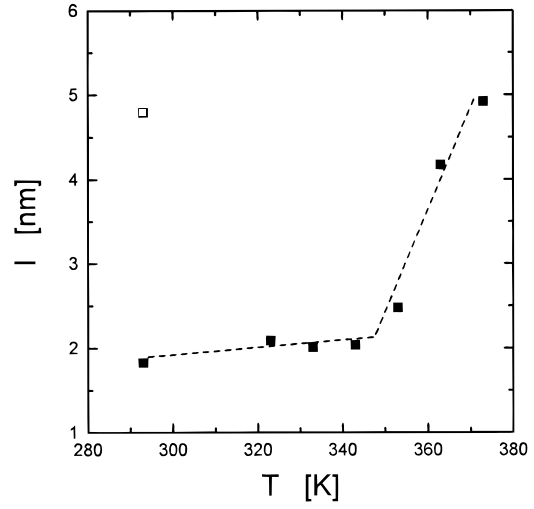

Figure 5. Temperature dependence of averaged characteristic length l of PCU/PMMA-IPN with 60 wt % PCU as determined from the coefficients of $S(q)$ (eq 17). The line is a guide for the eye.

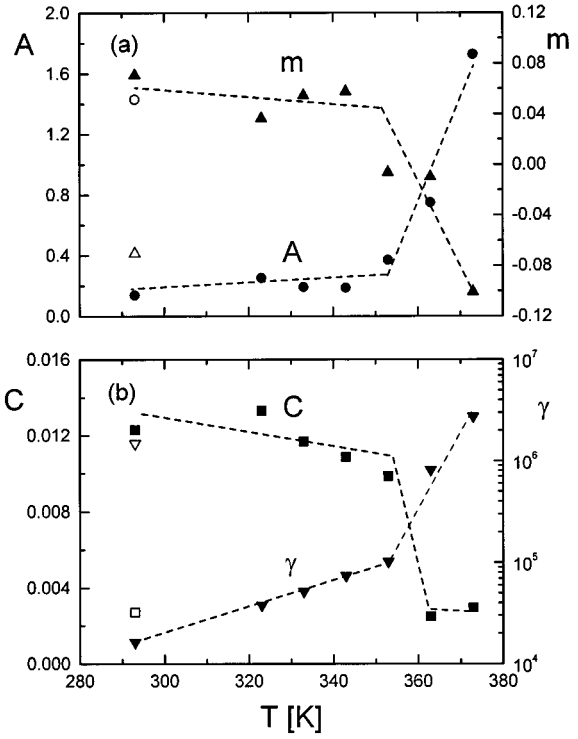

Figure 6. Temperature dependence of the coefficients of the hydrodynamic structure factor $S(q)$ (eq 15) of PCU/PMMA-IPN with 60 wt % PCU. The lines are guides for the eye.

able explanation for the lower temperature of unfreezing of the mobility of the PMMA network component compared to the bulk PMMA network ($T_g = 382$ K) is a plasticizing effect by the PCU component. Even on the scale of several nanometers the phases are not expected to be pure.

The temperature dependence of the coefficients $\bar{A}$, $\bar{m}$, $\bar{C}$, and γ are shown in Figure 6. All parameters show significant changes above 353 K. Although due to the time averaging during reaction and the additional temperature changes the parameters of the hydrodynamic theory have not a simple physical meaning, we attempt a rather qualitative discussion of the temperature dependence. The $\bar{C}$ parameter which reflects the topological constraints between the two different networks should either be constant or increase with tem-

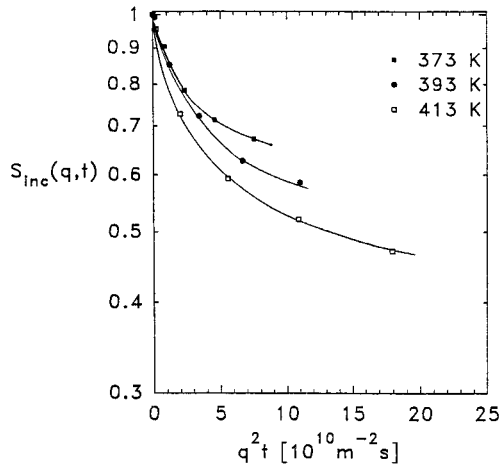

Figure 7. Echo attenuation plot $S_{inc}(q'^2t)$ at different temperatures of PCU/PMMA-IPN with 60 wt % PCU. The diffusion times t are 20 ms (373 K), 30 ms (393 K), and 50 ms (413 K). The lines are guides for the eye.

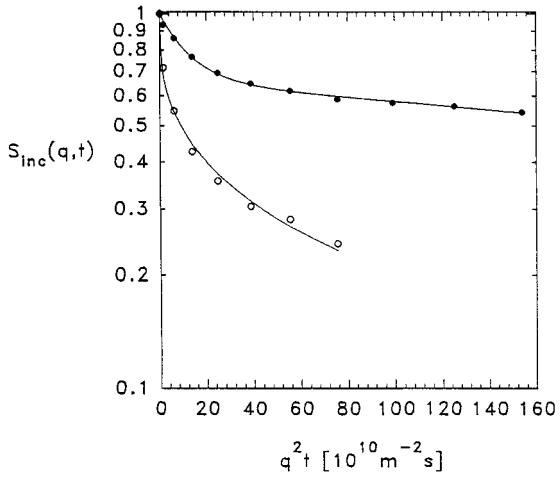

Figure 8. Echo attenuation plot $S_{inc}(q'^2t)$ measured at T = 413 K with (●) and without (○) preheating (3 h at 413 K) of PCU/PMMA-IPN with 60 wt % PCU. The lines are fits which are explained in the text.

perature because of the increasing restriction by a thermally driven demixing process in the IPN. On the other hand, it is expected that the frozen composition fluctuations become less restricted at the small scale glass transition of one of the components, which is similar to cutting some of the loops of the IPN. The value of $\bar{C}$ should then be drastically reduced, which is seen in Figure 6a. The parameter γ which is a measure for the mobility is strongly increased above 353 K (see Figure 6a), as expected for unfreezing of the degrees of freedom of the PMMA network components. For the case of a lower critical spinodal temperature the difference $\chi_c - \chi$, which reflects $T_c - T$, should become smaller with increasing temperature. This effect should be again more drastic above the short range glass transition, where the frustrated structure can at least partially equilibrate. This suggested decrease is found above 353 K for $\bar{m}$, which is proportional to $\chi_c - \chi$. From eq (16) it is seen that even small negative values of $\bar{m}$ are allowed. The temperature dependence of $\bar{m}$ plotted in Figure 6b is consistent with this explanation. $\bar{A}$ also increases tremendously above 353 K, which is an indication for a differentiation in the structure of the IPN.

The irreversible changes of the IPN above the temperature of the small scale glass transition of the less flexible component may be due to further separation of the two interpenetrated network components in the direction of a lower free enthalpy of mixing, motion of free ends or free loops out of the second network component, and/or diffusion of small molecules trapped in the structure. All these structural changes can be pinned by a possible completion of the chemical reaction at higher temperatures, leading to an irreversibly bonded structure. The discussed changes in the averaged length and the coefficients of the theory are in agreement with all of these possibilities. The remaining irreversible contribution to the scattering intensity after cooling may be related to the suggested completion of the chemical reaction and the chemical frustration of the structure developed above the small scale glass transition.

This view finds partial support by temperature dependent field gradient NMR measurements on the same samples shown in Figures 7 and 8. Figure 7 shows the normalized intermediate incoherent scattering function $S_{inc}(q',t)$ for the sample with 60 wt % PCU. A reasonable signal is only obtained for higher temperatures ($T \geq 373$ K). This may be considered as a hint for a sharp change in molecular mobility at about 373 K, which corresponds to the suggested glass transition in the PMMA domains. The data reveal a rather broad distribution of self-diffusivities with "fast" (small molecules) and "slow" components (dangling ends, network chains, free long chains). The contribution of the "slow" components to the signal decreases with increasing observation time t due to its shorter relaxation time T_1 as compared to the "fast" components (see eq (6)). The contribution of the "fast" components to the signal is much larger than their fraction in the sample because the mobile components have long nuclear magnetic relaxation times. The overall fraction of mobile components in the sample is estimated to be several percent. An estimation of the self-diffusion coefficient of the more mobile species from the slope of the curves at $q'^2t \rightarrow 0$ gives a diffusion coefficient D_1 of about 4×10^{-11} m^2 s^{-1}, which is rather typical for small molecules in a polymer matrix (above T_g) than for free polymer chains. Figure 8 shows $S_{inc}(q',t)$ at 413 K and $t = 50$ ms without thermal treatment (the same as in Figure 7) and after annealing the sample at 393 K for 3 h. Whereas before thermal treatment we observe a broad distribution of self-diffusion coefficients in the sample (the fit in Figure 8 is a KWW fit with $D = 3.4 \times 10^{-12}$ m^2 s^{-1} and $\beta = 0.34$), after thermal treatment $S_{inc}(q',t)$ is almost bi-exponential ($D_1 = 8 \times 10^{-12}$ m^2 s^{-1}, $D_2 = 1 \times 10^{-13}$ $m^2 s^{-1}$) with a clearly observable slow self-diffusion process and a strongly reduced contribution of mobile species. The overall fraction of mobile components after temperature treatment can be approximated to be below 1%. The decrease of the fraction of the mobile species of the network is some evidence of the continuation of the chemical reaction of the simultaneous IPN at high temperatures, which leads to a pinning of the developed structure.

Conclusions

We measured the composition and temperature dependence of the scattering profiles of finely microphase dispersed IPNs. The scattering curves at room temperature were fitted by the Debye−Bueche theory and a structure factor obtained in the hydrodynamic limit for simultaneously cross-linked IPNs. The curves are in good agreement with these theories. The averaged

parameters of the hydrodynamic theory reflect the characteristic length of the composition fluctuations, the topological restraints between the network components, and the tendency for phase separation. The characteristic lengths for different compositions are found to vary from 2 to 35 nm. For the sample with 60 wt % PCU the temperature dependence of scattering intensity has been studied between 298 and 373 K. The scattering intensity at small q values increases slightly with increasing temperature. Above 353 K the scattering intensity increases tremendously and a maximum at q^* becomes evident. The maximum in scattering intensity cannot be described by the Debye−Bueche theory, whereas it is in agreement with the hydrodynamic structure factor. It was found that all the parameters change tremendously above a temperature of 353 K. The correlation length of the structure increases by a factor of about 2. These changes are considered to be due to a small scale glass transition in the PMMA network component which unfreezes the frustrated structure. This is also evidence that, besides the topological restraints by chemical cross-links and entanglements, the composition fluctuations have been frustrated by the vitrification of the PMMA component. The changes of the structure factor above 355 K are assumed to reflect further separation of the interpenetrated network components and/or the diffusion of free ends, free loops, or small molecules out of the second component of the network. From the remaining irreversible changes of the structure factor after cooling to room temperature and the decrease of the fraction of small molecules found in the pulsed field gradient NMR experiments, we assume a pinning of the irreversible structural changes after annealing.

Acknowledgment. This work has been supported by the Bundesminister für Wirtschaft through the Arbeitsgemeinschaft Industrieller Forschungsvereinigungen e.V., Grant No. 10517 and the National Science Foundation, Grant No. DMR-9628224. I.A. thanks the Deutsche Forschungsgemeinschaft for travel expenses.

References and Notes

(1) Sperling, L. H. *Interpenetrating Polymer Networks and Related Materials*; Plenum: New York, 1981.
(2) Frisch, H. L. *Br. Polym. J.* **1985**, *17*, 149.
(3) Lipatov, Y. S. In *Advances in Interpenetrating Networks*; Klempner, D., Frisch, K. C., Eds.; Technomic: Lancaster, 1989; Vol. I.
(4) Koberstein, J. T.; Stein, R. S. *Polym. Eng. Sci.* **1984**, *24*, 293.
(5) McGarey, B. In *Advances in Interpenetrating Networks;* Klempner, D., Frisch, K. C., Eds.; Technomic: Lancaster, 1989; Vol. I.
(6) Brulet, A.; Daoud, M.; Zhou, P.; Frisch, H. L. *J. Phys. II Fr.* **1993**, *3*, 1161.
(7) Lee, D. S.; Kim, S. C. *Macromolecules* **1984**, *17*, 2193 and references therein.
(8) Alig, I.; Junker, M.; Schulz, M.; Frisch, H. L. *Phys. Rev. B* **1996**, *53* (17), 11481.
(9) Debye, P.; Bueche, A. M. *J. Appl. Phys.* **1949**, *20*, 518.
(10) Debye, P.; Anderson, H.; Brumberger, H. *J. Appl. Phys.* **1957**, *28*, 679.
(11) Porod, G. *Kolloid Z.* **1951**, *124*, 83; **1952**, *125*, 51; **1952**, *125*, 108.
(12) deGennes, P. G. *Scaling Concepts in Polymer Physics*; Cornell: Ithaca, NY, 1979.
(13) Schulz, M. *J. Chem. Phys.* **1992**, *97*, 5631.
(14) Leibler, L. *Macromolecules* **1980**, *13*, 1602.
(15) Frisch, H. L.; Zhou, P.; Frisch, K. C.; Xiao, X. H.; Huang, M. W.; Ghiradella, H. *J. Polym. Sci., Part A: Polym. Chem.* **1991**, *29*, 1031.
(16) Strobl, G. *Acta Crystallogr.* **1970**, *A26*, 367.
(17) Wiegand, W.; Ruland, W. *Colloid Polym. Sci.* **1979**, *66*, 355.
(18) Baltà-Calleja, F. J.; Vonk, C. G. In *X-Ray Scattering of Synthetic Polymers*; Jenkins, A. D., Ed.; Elsevier: New York, 1989.
(19) Kärger, J.; Fleischer, G. *TrAC* **1994**, *13*, 145.
(20) Flory, P. J. *Principles of Polymer Chemistry*; Cornell: Ithaca, NY, 1953.
(21) deGennes, P. G. *J. Phys. Lett. (Paris)* **1979**, *40*, L-69.
(22) Bettachy, A.; Derouiche, A.; Benhamou, M.; Daoud, M. *J. Phys.* **1991**, *1*, 153.
(23) Stepanow, S.; Schulz, M. *J. Chem. Phys.* **1993**, *98*, 6558.
(24) Doi, M.; Edwards, S. F. *Theory of Polymer Dynamics;* Wiley: New York, 1987.
(25) Schulz, M.; Frisch, H. L. *J. Chem. Phys.* **1994**, *101*, 10008.
(26) Lal, J.; Widmaier, J. M.; Bastide, J.; Boué, F. *Macromolecules* **1994**, *27*, 6443.
(27) Schulz, M.; Frisch, H. L. *Phys. Rev. B*, in press.

MA9610469